processes

MDPI

Article

Research on Heat Transfer Performance of Cold-Water Pipe in Ocean Thermal Energy Conversion System

Jing Li [1], Bo Ning [1,*], Lele Yang [2], Fenlan Ou [1], Bo Li [3], Dezhi Qiu [1] and Xuemei Jin [1]

[1] Guangzhou Marine Geological Survey, China Geological Survey, Guangzhou 511458, China
[2] School of Civil Engineering and Transportation, South China University of Technology, Guangzhou 510641, China
[3] Guangdong Nanyou Holding Group Co., Ltd., Guangzhou 510075, China
* Correspondence: 15022401058@139.com; Tel.: +86-15022401058

Abstract

Ocean Thermal Energy Conversion (OTEC) is characterized by its abundant reserves and pollution-free nature, enabling stable power generation around the clock. Since the power output of an OTEC system is significantly influenced by the energy available from cold and warm seawater, the accurate evaluation of the outlet temperature of the cold-water pipe (CWP) is crucial. To analyze the heat transfer performance of the CWP, this paper investigates the temperature field of the OTEC CWP and employs numerical simulation methods to conduct finite element analysis of the temperature field under different discharge conditions. The results indicate that during the pumping of deep-sea cold water through the CWP, heat is absorbed from the warmer upper seawater layers. When the pumping discharge rate is higher, the shorter fluid residence time due to higher flow velocity results in a lower outlet temperature. Compared to steel CWPs, high-density polyethylene (HDPE) is more suitable for OTEC systems due to its lower thermal conductivity and density.

Keywords: ocean thermal energy conversion; cold-water pipe; analysis of pipe temperature; finite element analysis

1. Introduction

Ocean Thermal Energy Conversion (OTEC) is a promising renewable energy technology that operates on the principle of harnessing the temperature differential between warm surface seawater and cold deep-sea water to generate electricity through thermodynamic cycles [1]. Distinguished by minimal power output fluctuations, OTEC can effectively compensate for the intermittent nature of solar and wind power generation [2,3]. Furthermore, when integrated with cooling applications, freshwater production, and mariculture, it enables a combined "power–cooling–freshwater–aquaculture" quadruple generation model. This integrated approach holds significant importance for achieving self-sufficient energy and resource supply on islands, potentially replacing diesel generators. It is projected to reduce the levelized cost of electricity from USD 0.5/kWh to USD 0.18/kWh, positioning OTEC as a multi-energy complementary hub for deep-sea development [4]. However, its commercial expansion remains constrained by high capital costs characteristic of utility-scale projects [5,6].

OTEC systems utilize the temperature gradient between warm surface seawater (typically 25–30 °C) and cold deep-sea water (approximately 4–6 °C at depths of 800–1000 m) to drive a thermodynamic cycle and generate electricity, seen in Figure 1. Conventional

Check for updates

Academic Editor: Ireneusz Zbicinski

Received: 12 March 2026
Revised: 30 March 2026
Accepted: 9 April 2026
Published: 10 April 2026

 https://doi.org/10.3390/pr14081223

OTEC systems typically employ the Rankine or Kalina cycle, using high-capacity seawater pumps to transport large volumes of warm and cold water to shore-based or platform-mounted power stations for heat exchange. Although these systems have demonstrated power-generation capacities of up to 1 MW, their scalability faces inherent limitations. For instance, the substantial energy consumption required for long-distance seawater extraction significantly reduces the net power output and economic viability. Among these challenges, the cold-water pipe (CWP) structure is relatively complex, involves high installation costs, and is susceptible to damage from ocean currents, wave action, and biofouling, thereby increasing operational and maintenance difficulties. Furthermore, the small temperature difference of only 20–25 °C limits the theoretical Carnot efficiency to approximately 6.7%, making OTEC power-generation efficiency highly sensitive to the CWP's structure and heat loss. In response, researchers have conducted dedicated studies on OTEC application models and related technologies [7–10], proposing future application prospects for OTEC systems. In terms of experimental applications, Guangzhou Marine Geological Survey of the China Geological Survey developed a 20 kW OTEC prototype. In July 2023, it was successfully tested aboard the "Hai Yang Di Zhi Er Hao" research vessel in the South China Sea [11]. The prototype utilized a steel CWP deployed to a depth of 840 m where the water temperature was 5.2 °C. By extracting deep seawater at a flow rate of 180 m^3/h, the CWP outlet temperature was maintained at approximately 6.23 °C, achieving a maximum power output of 16.4 kW and validating the feasibility of ocean thermal energy conversion for power generation. The 20 kW OTEC prototype devices seen in Figure 2.

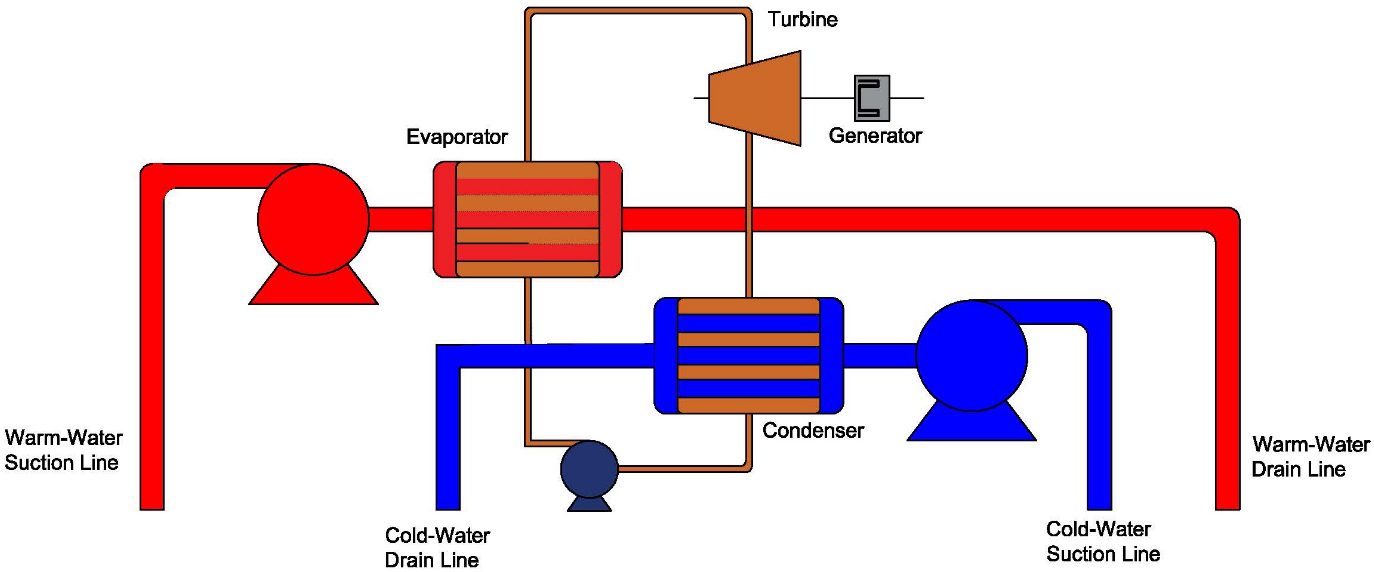

Figure 1. Diagram of OTEC.

The aforementioned CWP represents one of the most challenging components in floating structures. For commercial development applications, where seawater flow velocities can reach 1–1.5 m/s, variations in internal flow rates during operation may lead to CWP failure [12,13]. Consequently, numerous researchers have conducted comprehensive studies focusing on OTEC CWPs and marine risers, investigating their structural mechanics [14–17], vortex-induced vibration [18–20], and fatigue fracture [21–23]. These studies have analyzed various factors affecting CWP stability in both frequency and time domains, including flow field conditions, flow direction, and centrifugal forces, ultimately providing recommendations for optimal CWP materials [24].

https://doi.org/10.3390/pr14081223

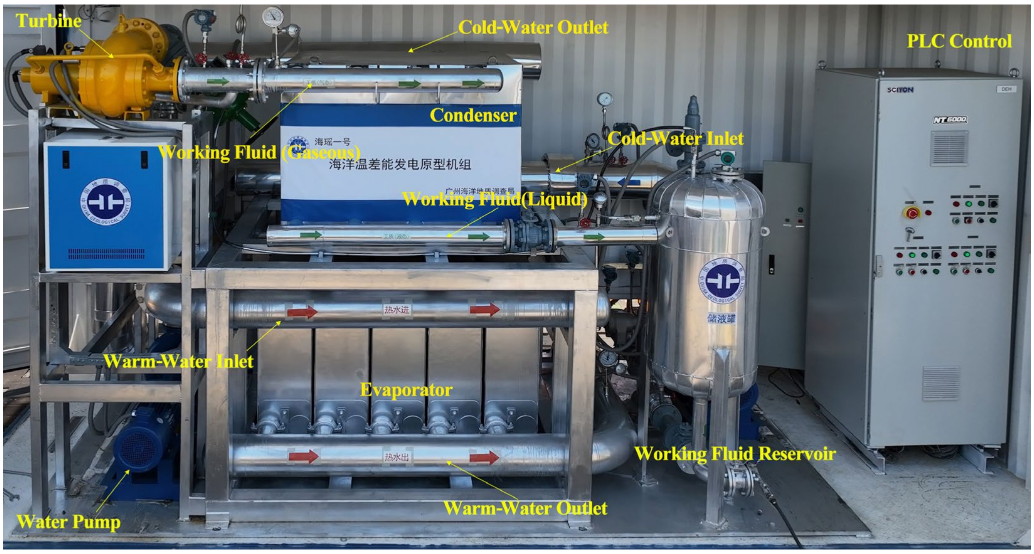

Figure 2. 20 kW OTEC prototype device.

However, in the OTEC systems, the thermal transfer efficiency of the CWP is a critical factor affecting overall system performance. Studies indicate that a mere 0.5 °C temperature rise along the CWP can reduce overall power-generation efficiency by over 1% [25,26]. This has prompted extensive research on enhancing CWP thermal performance. For instance, Fan et al. [27] developed a thermo-economic model for OTEC systems, aiming to optimize both thermodynamic and economic performance. Their study examined how warm seawater temperature and cold seawater depth affect net thermal efficiency and total investment cost. Thirugnana et al. [7] assessed Malaysia's OTEC potential using oceanographic data, establishing a thermodynamic balance system for a 10 MW Rankine-cycle OTEC plant. The system combined plate heat exchangers with anhydrous ammonia, achieving a net power output representing 70–80% of gross generation. Firmansyah et al. [28] applied the finite volume method to model temperature distribution along the CWP, predicting temperature rise in cold seawater during transport through numerical simulations based on mass and heat transfer principles. Fu Qiang et al. [29] created an analytical model for temperature field distribution in CWPs deployed from floating platforms. Using finite volume discretization and solution methods, they characterized temperature distribution patterns in OTEC CWPs. Zhang Jichang [30] employed theoretical calculations and finite element analysis to investigate temperature variations in "gap-casing" composite CWPs, examining how interlayer materials influence thermal performance. Mao et al. [31] established a numerical model analyzing temperature distribution and heat transfer characteristics along CWPs during deep seawater extraction. Their finite volume method solution explored the impacts of CWP material, wall thickness, flow rate, and insulation thickness on outlet temperature.

Although the computational simulation method for the CWP temperature enables the simulation of the pipe column along its length, the complexity of such an approach hinders its widespread adoption. Based on a 20 kW OTEC system's CWP, this paper employs finite element analysis to simulate the temperature field during the water intake process, taking into account variables such as the seawater temperature along the path and ocean current velocity. A detailed investigation is conducted into the effects of flow rate and pipe column type on the outlet water temperature. The aim is to provide an efficient and convenient means of evaluating the intake water temperature of the CWP in OTEC systems, thereby offering a theoretical foundation for OTEC design, CWP column selection, and system thermal efficiency analysis.

2. OTEC CWP Temperature Model

The CWP, typically installed on OTEC systems, functions as a critical component to supply deep-sea cold water to the floating platform. Power generation is achieved by harnessing the temperature differential between the deep cold water and warm water. The CWP is suspended from the power-generation unit on the floating platform at its top end, while its bottom end is secured to the seafloor via anchors. Deep seawater is pumped to the surface through top-mounted or subsea pump systems. The overall process flow is illustrated in Figure 3.

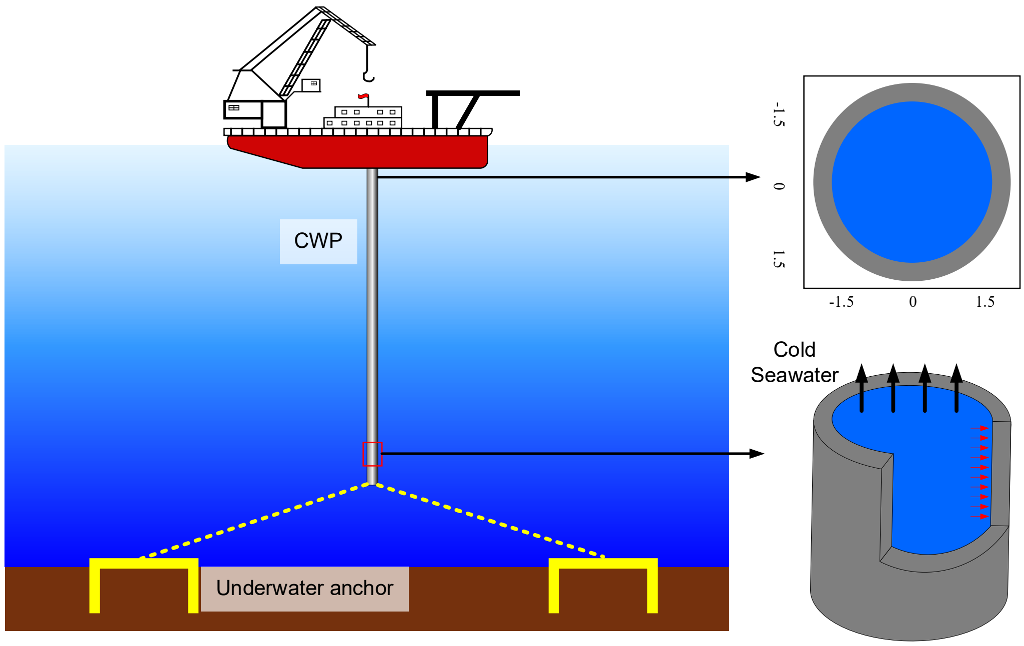

Figure 3. Diagram of CWP water intake.

The main nomenclature is determined in Table 1.

Table 1. Nomenclature.

Parameter	Meaning	Unit
ρ	fluid density	kg/m^3
A	pipe's cross-sectional area	m^2
u	fluid velocity	m/s
C_p	specific heat capacity at constant pressure	J/(kg·K)
T	temperature	K
k	thermal conductivity	W/(m·K)
f_D	Darcy friction factor	-
Z	pipe perimeter	m
h	overall heat transfer coefficient	$W/(m^2 \cdot K)$
T_{ext}	external ambient temperature	K
r_n	outer radius of the pipe wall	m
h_{int}	internal film heat transfer coefficient	$W/(m^2 \cdot K)$
h_{ext}	external film heat transfer coefficient	$W/(m^2 \cdot K)$
k_n	thermal conductivity of the pipe wall	W/(m·K)
d	pipe outer diameter	m

During the water extraction process in an OTEC system, deep cold seawater flows upward through the CWP, during which heat exchange occurs between the cold fluid inside the pipe and the external fluid. The following assumptions are made regarding this process:

https://doi.org/10.3390/pr14081223

the seawater within the CWP follows a one-dimensional flow pattern; compression effects, density variations, and flow velocity changes in the seawater inside the pipe are neglected; and the heat transfer during upward flow is considered steady-state.

As the cold seawater inside the CWP moves upward, several energy factors must be considered: its internal energy, convective heat transfer between the seawater and the pipe wall, energy changes due to mass transfer during flow, and heat generated by fluid friction. The energy equation governing the seawater flow within the CWP is given as follows [32]:

$$\rho A C_p u \cdot \nabla T = q_s + Q_{wall} \tag{1}$$

In the equation above, q_s represents the sum of heat fluxes from convection and radiation. For the CWP, this can be expressed by the following equation:

$$q_s = \nabla \cdot Ak\nabla T + f_D \frac{\rho A}{2d_h}|u|^3 \tag{2}$$

Q_{wall} represents the source/sink term for heat exchange through the pipe wall with the surrounding environment, expressed as follows:

$$Q_{wall} = hZ(T_{ext} - T) \tag{3}$$

For cylindrical pipes, considering uniform surrounding temperature and quasi-static heat transfer through the pipe wall, the effective hZ in Equation (3) is given by the following:

$$(hZ)_{eff} = \frac{2\pi}{\frac{1}{r_0 h_{\text{int}}} + \frac{1}{r_N h_{ext}} + \sum_{n=1}^{N}\left(\frac{\ln(\frac{r_n}{r_n - 1})}{k_n}\right)} \tag{4}$$

The internal film resistance is defined as follows [33]:

$$h_{\text{int}} = Nu_{\text{int}} \frac{k}{d} \tag{5}$$

The Nusselt number correlation in the above equation is as follows:

$$Nu_{\text{int}} = \frac{\frac{f_D}{8}(\text{Re} - 1000)\text{Pr}}{1 + \sqrt{12.7}(\text{Pr}^{2/3} - 1)} \tag{6}$$

The film resistance caused by the surrounding seawater is as follows:

$$h_{ext} = Nu_{ext} \frac{k}{d} \tag{7}$$

For forced convection conditions, the Nusselt number correlation adopts the following form:

$$Nu_{ext} = 0.3 + \frac{0.62\sqrt{\text{Re}}\text{Pr}^{1/3}}{\left[1 + (0.4/\text{Pr})^{2/3}\right]^{1/4}}\left[1 + (\text{Re}/282000)^{5/8}\right]^{4/5} \tag{8}$$

3. Finite Element Modeling and Verification

Based on practical considerations, a CWP model, was established. Numerical simulations were conducted to perform finite element analysis of the temperature field under six different discharge conditions. The CWP specifications correspond to a 1 MW installed capacity OTEC system, with a cold-water intake depth of 1000 m and vertical deployment in the ocean. The study also analyzes the effects of three different pipe materials on

https://doi.org/10.3390/pr14081223

temperature distribution along the pipeline. Parameters relevant to simulating the water extraction process in OTEC CWPs are summarized in Table 2.

Table 2. Simulation parameters.

Parameters	Value
Outer diameter of CWP, m	1.35
Thickness of CWP, mm	38.1
Material of CWP	Steel Steel with an insulation layer High-density polyethylene (HDPE)
Surface temperature of seawater, °C	31.2
Temperature at the intake location, °C	3.5
Specific heat capacity of seawater, J/(kg·K)	4185
The thermal conductivity of seawater, W/(m·K)	0.59
Pump rate, m^3/h	2000, 4000, 6000, 8000, 10,000, 12,000

Figure 4 illustrates the seawater temperature distribution in a specific marine area. As shown in the figure, the sea surface temperature during summer is approximately 31.2 °C. The temperature gradually decreases with increasing depth, reaching about 3.5 °C at around 1000 m. Thus, this temperature profile is adopted as the initial condition in this study, implying that when the CWP is immersed in seawater, the pipe and the internal seawater maintain the same temperature as the external ambient seawater, and no temperature difference exists.

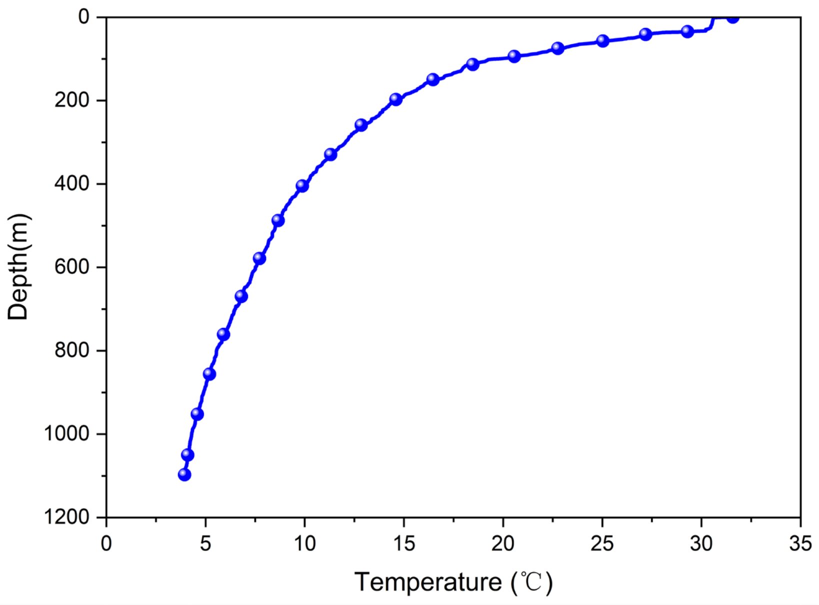

Figure 4. Temperature distribution of seawater.

Ocean currents, through convective heat transfer effects, can significantly enhance the heat transfer capacity of marine pipes, thereby increasing the temperature distribution along the flow path. This constitutes a critical factor that cannot be neglected in temperature simulations. The variation in ocean current velocity with depth in the calculations of this study is described by the following equation [34,35]:

$$U_c(z) = U_{c0}\left(\frac{z+d}{d}\right)^{\frac{1}{7}} \tag{9}$$

where $U_c(z)$ represents the current velocity at depth z ($z \leq 0$); U_{c0} denotes the surface current velocity (z = 0), taken as 0.48 m/s after linear superposition considering a wind speed of 6 m/s and a tidal current velocity of 0.35 m/s; z is the vertical coordinate, defined as positive upwards from the still water level; and d is the water depth. The ocean current velocities under different depth conditions are shown in Figure 5 below.

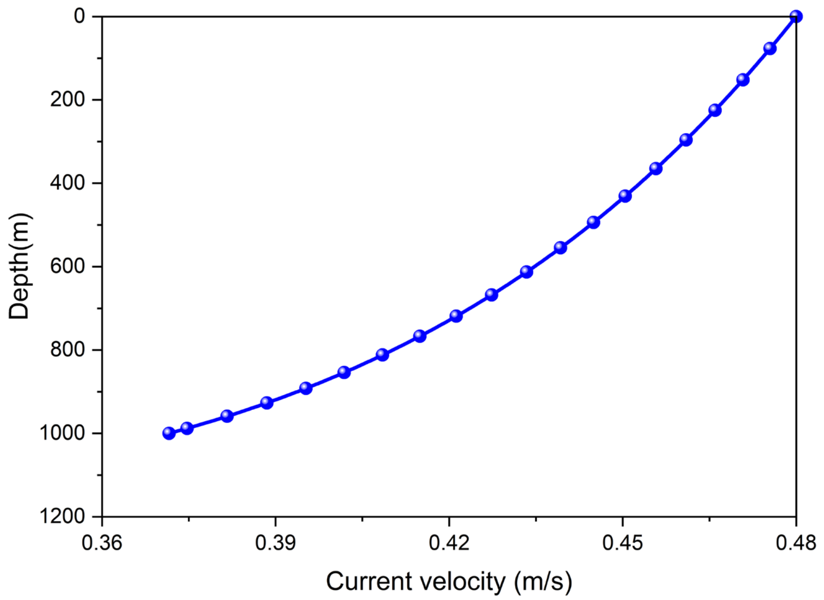

Figure 5. Velocity distribution of seawater.

To validate the accuracy of the aforementioned finite element model, the present model was employed to calculate the temperature distribution along the CWP of the 20 kW OTEC system during its sea trial in July 2023. The configuration of the cold- and warm-water pipes during the sea trial is shown in Figure 6.

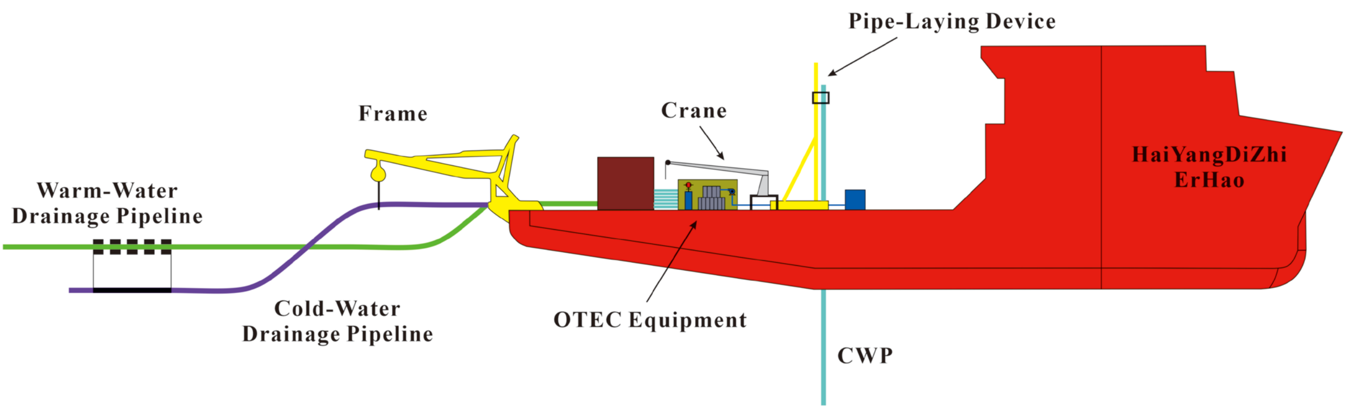

Figure 6. Schematic diagram of OTEC.

In the depicted setup, the cold-water pipe is constructed of steel with an outer diameter of 245 mm, an inner diameter of 220 mm, and a total length of 840 m. The intake water temperature was 5.2 °C, while the surface seawater temperature was 26 °C. All other parameters remained consistent with the experimental conditions. A comparison between the model-predicted temperature variations along the pipe at different depths and the measured outlet temperature from the OTEC sea trial is presented in Figure 7. The results demonstrate close agreement between the simulated and measured data: the model predicts an outlet temperature of 6.17 °C, which closely matches the experimentally measured value of 6.2 °C from the OTEC sea trial, merely a 0.48% error. This correlation validates the accuracy of the proposed model.

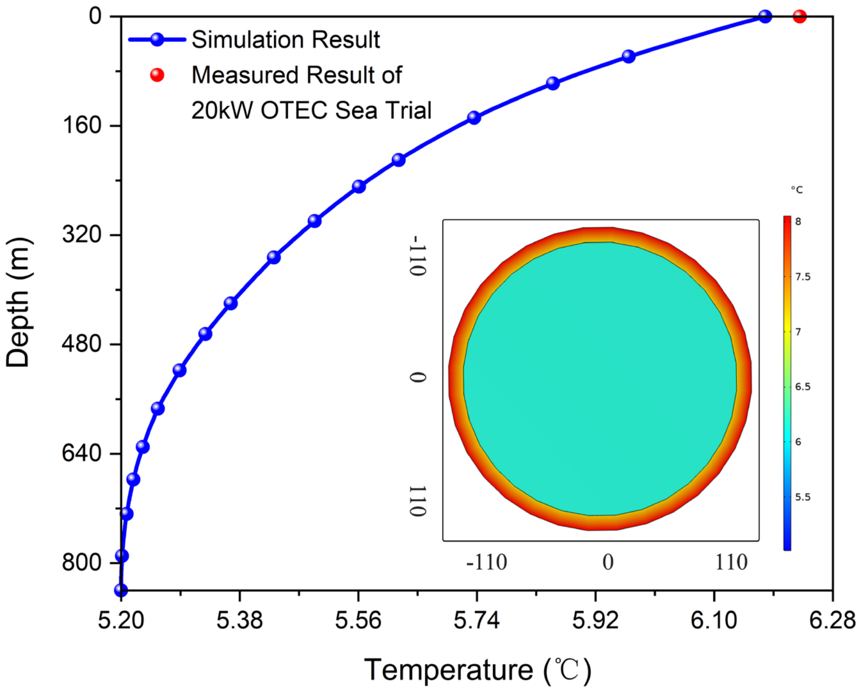

Figure 7. Comparison between finite element simulation results and actual temperature.

4. Analysis of Temperature Characteristics of CWP

Simulation of temperature distribution during deep seawater extraction through the CWP in an OTEC system was conducted using the pipe specifications and parameters listed in Table 2. Under prolonged operation conditions, the steady-state temperature field of the pipe was considered while analyzing the effects of different materials and discharge rates on the temperature variation in seawater inside the CWP. Figures 8 and 9 illustrate the temperature rise and outlet temperature distribution of the steel CWP under different discharge rates. Figure 8 demonstrates that the seawater temperature inside the pipe decreases significantly with increasing discharge rate. This phenomenon occurs because higher discharge rates lead to increased flow velocity within the pipe, consequently reducing the heat exchange duration between the internal seawater and the external environment. The reduced heat loss results in lower outlet seawater temperature.

Figure 9 presents the nephogram of the temperature field variation at the CWP outlet. The figure reveals a relatively uniform temperature distribution inside the pipe, with significant temperature changes occurring only at the outer wall. This indicates minimal heat absorption from external seawater during the cold-water extraction process, resulting in negligible temperature fluctuations inside the pipe. Furthermore, due to the cooling effect of the internal cold seawater, the temperature at the pipe's outer wall remains lower than the surface seawater temperature.

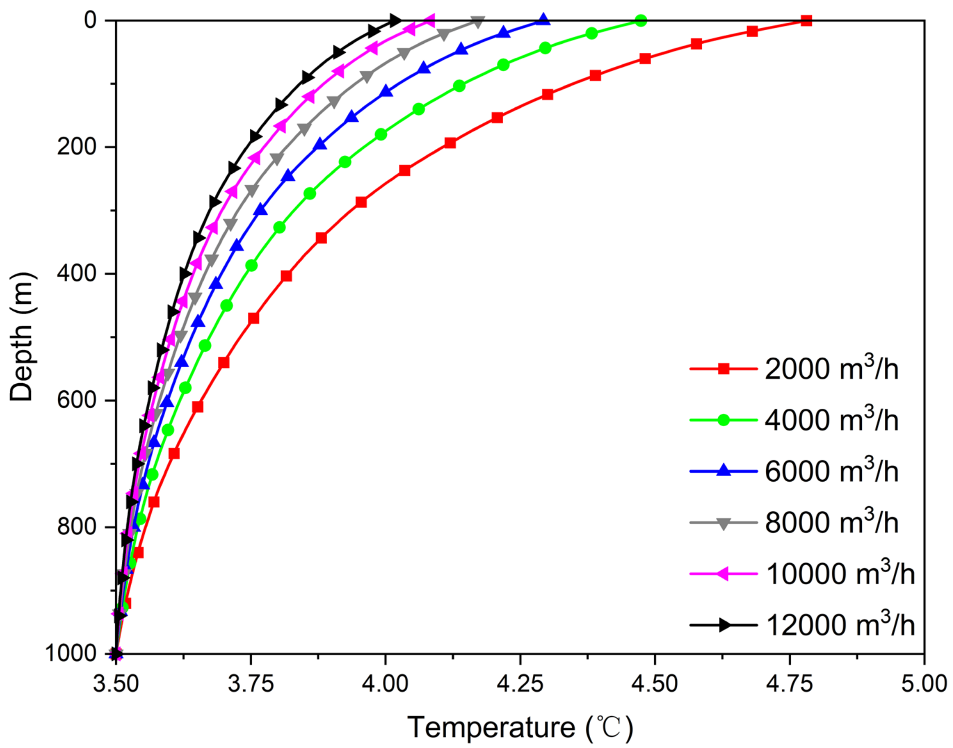

Figure 8. Effect of discharge rate on temperature in steel CWP.

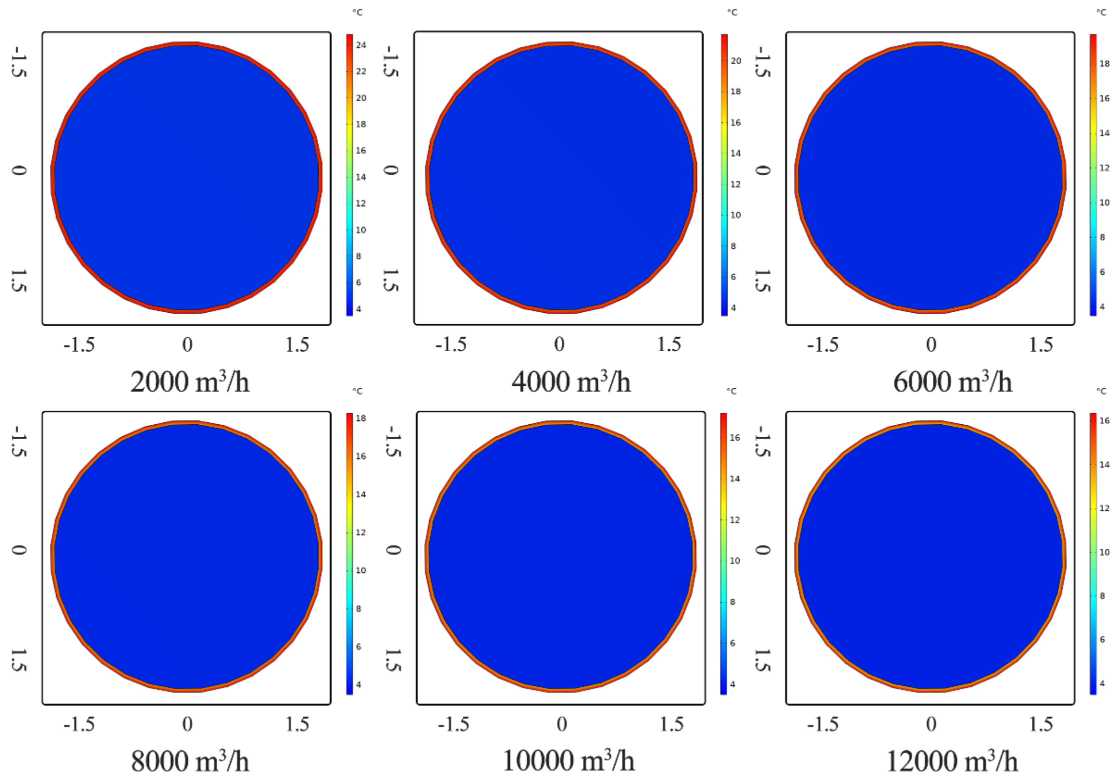

Figure 9. Outlet temperature of steel CWP under different discharge rates.

As shown in Table 3, when the discharge rate remains at relatively low values (e.g., 2000 m^3/h), the temperature increase is approximately 1.28 °C, corresponding to a 36.6% temperature rise rate. When the discharge rate increases to 12,000 m^3/h, the temperature increase reduces to 0.516 °C, with the temperature rise rate decreasing to 14.75%. The significant reduction in temperature fluctuation along the pipeline indicates that large discharge rates can maintain the internal temperature within a narrow range, ensuring stable outlet temperature and providing sufficient cold source for the system.

Table 3. Effect of discharge rate on outlet temperature of steel CWP.

Rates, m^3/h	Outlet Temperature, °C	Temperature Rise, °C	Rise Rate, %
2000	4.781	1.281	36.60
4000	4.474	0.974	27.83
6000	4.293	0.793	22.66
8000	4.171	0.671	19.18
10,000	4.083	0.583	16.67
12,000	4.016	0.516	14.75

Figures 10 and 11 display the temperature rise and outlet temperature distribution of the high-density polyethylene (HDPE) CWP under different discharge rates. The temperature distribution pattern in Figure 10 confirms that the temperature variation inside the HDPE pipe follows the same trend as the steel pipe, with seawater temperature decreasing significantly as discharge rate increases, further validating the conclusion that large discharge rates reduce outlet temperature.

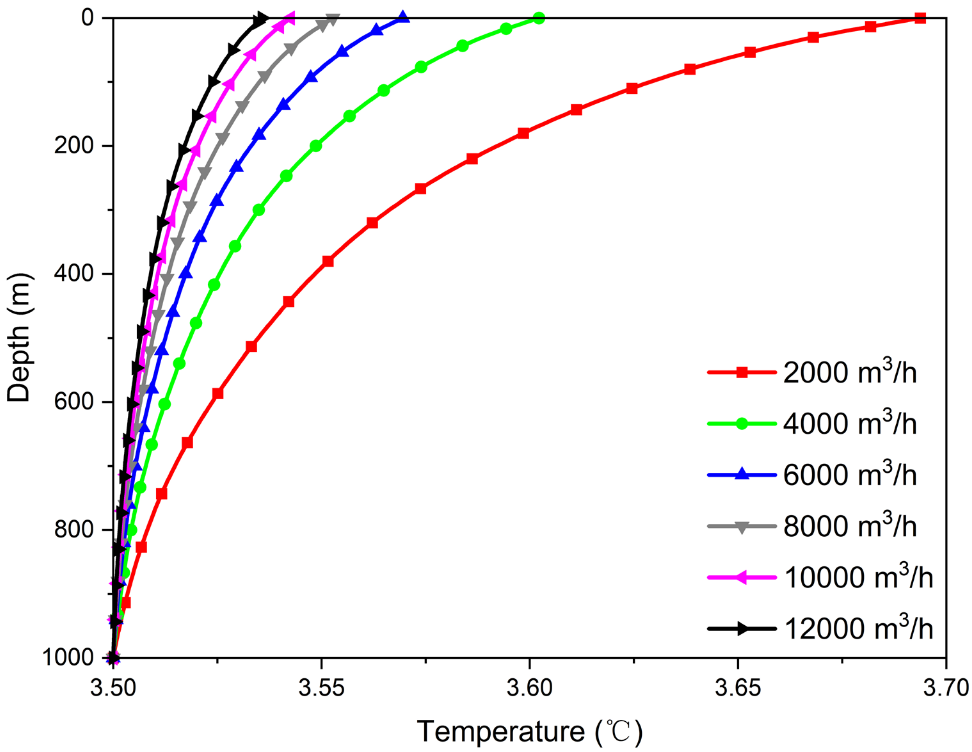

Figure 10. Effect of discharge rate on temperature in HDPE CWP.

Figure 11 shows the nephogram of temperature field variation at the HDPE CWP outlet. The uniform internal temperature distribution, combined with HDPE's lower thermal conductivity compared to steel, results in the outer-wall temperature being closer to the ambient seawater temperature while the internal temperature gradually decreases. This verifies the conclusion that minimal heat absorption from external seawater causes negligible internal temperature fluctuations. The outer-wall temperature also remains closer to the surface seawater temperature.

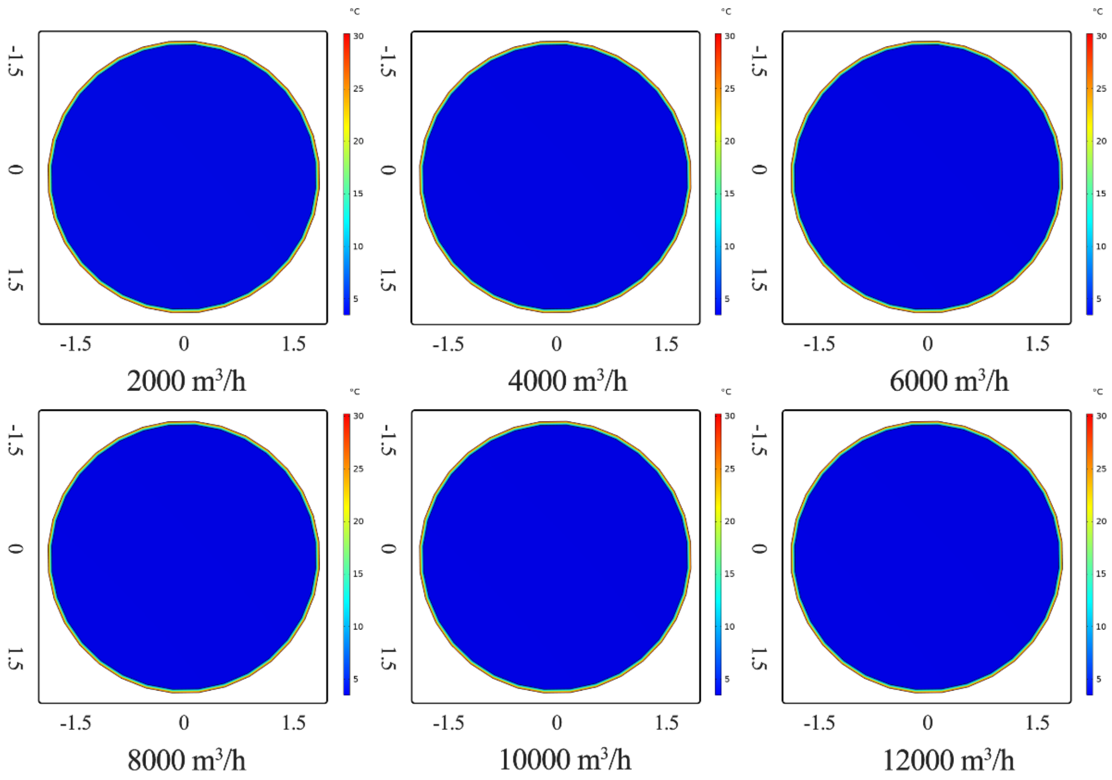

Figure 11. Outlet temperature of HDPE CWP under different discharge rates.

Table 4 demonstrates that even at low discharge rates (2000 m^3/h), the temperature increase is merely 0.194 °C with a 5.54% rise rate. At 12,000 m^3/h, the temperature increase reduces to 0.036 °C with only 1.02% rise rate. This indicates that even at low discharge rates, the CWP outlet temperature can be maintained at very low levels, providing an adequate cold source for the power-generation system.

Table 4. Effect of discharge rate on outlet temperature of HDPE CWP.

Rates, m^3/h	Outlet Temperature, °C	Temperature Rise, °C	Rise Rate, %
2000	3.694	0.194	5.54
4000	3.602	0.102	2.92
6000	3.570	0.070	1.99
8000	3.553	0.053	1.51
10,000	3.543	0.043	1.22
12,000	3.536	0.036	1.02

The study also analyzed steel CWPs with external insulation layers, as shown in Figures 12 and 13. Figure 12 reveals that efficient insulation significantly reduces outlet temperature, maintaining temperature rise below 0.015 °C across all discharge rates, outperforming both steel and HDPE configurations.

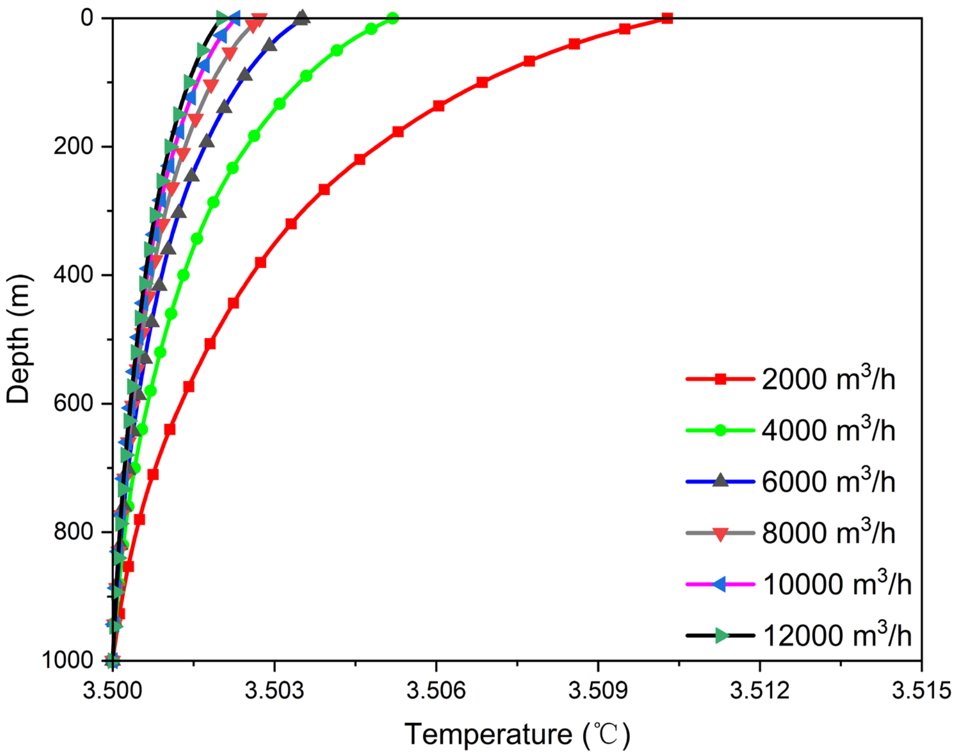

Figure 12. Effect of discharge rate on temperature in steel with external insulation layers CWP.

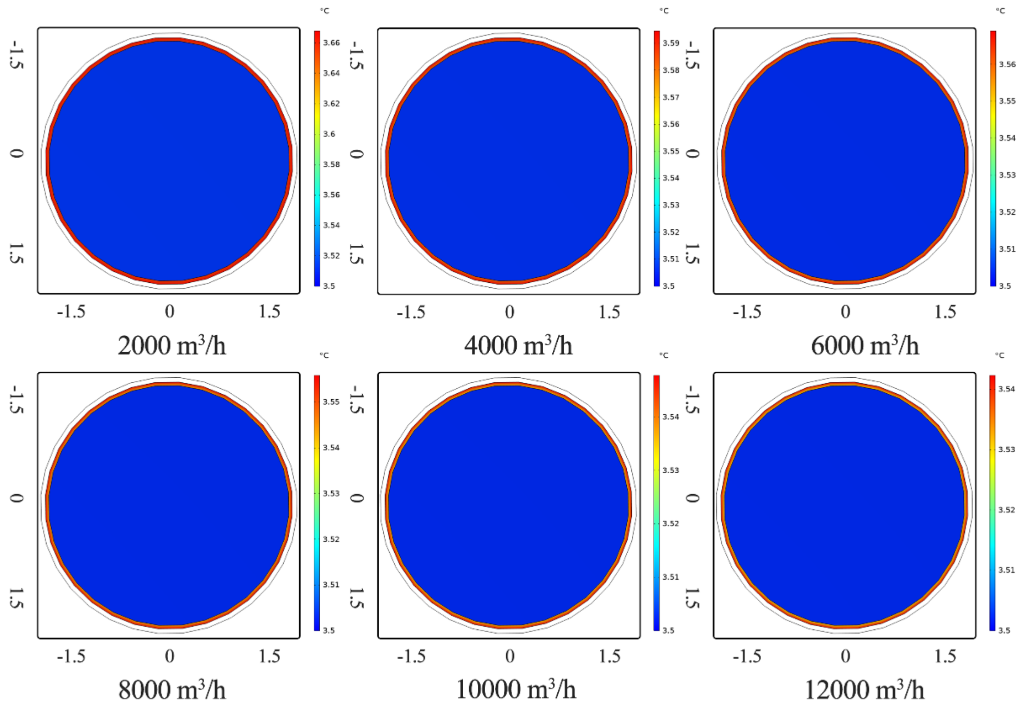

Figure 13. Outlet temperature of steel with external insulation layers CWP under different discharge Rates.

Figure 13 presents the nephogram of the temperature field variation at the outlet of the insulated steel CWP. The thermal barrier provided by the insulation maintains low and uniform pipe temperature, showing minimal difference from the internal seawater temperature, representing the lowest temperature among the three configurations.

As indicated in Table 5, when using large discharge rates (12,000 m^3/h) for deep seawater extraction, the outlet temperature increases by only 0.002 °C with a mere 0.06%

rise rate. Even at lower discharge rates (2000 m^3/h), the temperature rise remains at 0.01 °C, significantly lower than both steel and HDPE configurations.

Table 5. Effect of discharge rate on outlet temperature of steel with external insulation layers.

Rates, m^3/h	Outlet Temperature, °C	Temperature Rise, °C	Rise Rate, %
2000	3.510	0.010	0.29
4000	3.505	0.005	0.15
6000	3.504	0.004	0.10
8000	3.503	0.003	0.08
10,000	3.502	0.002	0.07
12,000	3.502	0.002	0.06

As a critical component in OTEC systems, the design of the CWP must take into account various factors such as structural strength, corrosion resistance, ease of installation, and life-cycle cost. In summary, HDPE offers significant advantages in terms of cost and installation convenience; however, special attention should be paid to the risk of pipe column buckling. It is suitable for small- to medium-scale or demonstration OTEC systems. Steel pipe columns are superior in structural strength and deep-water reliability, capable of withstanding deep-water hydrostatic pressure and dynamic loads. Moreover, the reliability of steel pipes has been well validated in conventional marine engineering, making them suitable for large-scale commercial projects. Insulated steel CWP can theoretically improve thermal efficiency and shares the same mechanical properties as steel pipes. However, compared to steel pipes, it has higher costs and more complex installation procedures, necessitating a detailed cost–benefit analysis before engineering application.

Based on the principle of OTEC, the designed power output determines the required amount of warm surface seawater and the quantity of cold seawater needed to condense the working fluid. Therefore, while maintaining the required flow rate, keeping the cold-water outlet temperature as low as possible helps sustain the condensation temperature of the working fluid. From the above analysis, it can be observed that a higher flow rate of cold seawater contributes to maintaining a lower outlet temperature, primarily because a faster flow velocity within the pipe column significantly shortens the flow residence time, thereby reducing the duration of heat exchange between the fluid and the surrounding environment (such as the pipe wall or ambient seawater). However, a higher flow velocity typically corresponds to a higher Reynolds number, which tends to induce turbulent flow inside the pipe column and enhances convective heat transfer. Nonetheless, due to the rapid transit of the fluid, the cumulative heat exchange from inlet to outlet is reduced, resulting in less heat loss from the outlet fluid. Therefore, for high-power OTEC systems, it is necessary to develop higher-power seawater extraction equipment. Under the condition of maintaining high pump power, increasing the seawater flow rate helps preserve a lower outlet seawater temperature.

However, it is worth noting that while an increase in the flow velocity inside the cold-water pipe helps reduce heat absorption loss during transport, excessive pumping energy consumption will significantly offset the net power output and overall energy conversion efficiency of the OTEC system. Consequently, the flow velocity within the cold-water pipe must be optimized through a trade-off between heat loss suppression and pumping power penalty.

5. Conclusions

1. During the pumping of deep cold seawater through the cold-water pipe (CWP) in Ocean Thermal Energy Conversion systems, heat absorption occurs from the

warmer upper seawater layers, resulting in a gradual temperature increase along the pipe. Given the substantial flow rates involved, the temperature distribution remains uniform within the pipe core, with significant variations confined to the pipe wall region, albeit with minimal magnitude.

2. The pumping discharge rate directly influences the internal flow velocity, thereby modifying the heat exchange duration between the internal seawater and the external environment. This consequently affects the outlet temperature of the cold seawater. While increased discharge rates help maintain lower outlet temperatures for specific power-generation requirements, excessively high rates may lead to prohibitive energy consumption.
3. Compared to steel CWPs, HDPE pipes demonstrate superior thermal insulation properties due to their lower thermal conductivity. Although external insulation layers can further enhance thermal performance, steel pipes' substantial weight imposes greater demands on platform design and installation procedures. Consequently, HDPE emerges as the more suitable material for OTEC CWPs, offering an optimal balance between operational practicality and thermal insulation performance.

Author Contributions: Study planning, generation of ideas: J.L., L.Y.; informational and data analysis: B.N., B.L.; literature evaluation: F.O., X.J.; writing—review and editing: J.L., D.Q. All authors have read and agreed to the published version of the manuscript.

Funding: This research was funded by the Nansha District Science and Technology Project (Grant Number: 2024ZD008). This research is also funded by the China Geological Survey (Grant number: No. DD20230066, DD20242659).

Data Availability Statement: Data are contained within the article.

Acknowledgments: The authors would like to thank the reviewers for their many constructive suggestions and comments that helped improve the quality of the paper.

Conflicts of Interest: Author Bo Li was employed by the company Guangdong Nanyou Holding Group Co., Ltd. The remaining authors declare that the research was conducted in the absence of any commercial or financial relationships that could be construed as potential conflicts of interest.

References

1. Zhang, L.; Tan, J.; Zhang, Y.; Xu, J.; Huang, S.; Duan, Q.; Duan, M. Dynamics response analysis of a cold-water pipe for ocean thermal energy conversion under different boundary conditions. *J. Vib. Shock* **2023**, *42*, 59–68. [CrossRef]
2. Nihous, G. A Preliminary Investigation of the Effect of Ocean Thermal Energy Conversion (OTEC) Effluent Discharge Options on Global OTEC Resources. *J. Mar. Sci. Eng.* **2018**, *6*, 25. [CrossRef]
3. Khosravi, A.; Syri, S.; Assad, M.E.H.; Malekan, M. Thermodynamic and economic analysis of a hybrid ocean thermal energy conversion/photovoltaic system with hydrogen-based energy storage system. *Energy* **2019**, *172*, 304–319. [CrossRef]
4. Saadha, A.; Ishihara, K.N.; Ogawa, T.; Basu, S.; Okumura, H. Techno-Economic Analysis of Combined Onshore Ocean Thermal Energy Conversion Technology and Seawater Air Conditioning in Small Island Developing States. *Sustainability* **2025**, *17*, 4724. [CrossRef]
5. Trenggono, M.; Hidayat, R.R.; Cahyo, T.N.; Mahardiono, M.D.; Destrianty, A.D. An assessment Indonesia's Ocean Thermal Energy Conversion (OTEC) as an electrical energy resource. *IOP Conf. Ser. Earth Environ. Sci.* **2021**, *746*, 012041. [CrossRef]
6. Jung, J.Y.; Lee, H.S.; Kim, H.J.; Yoo, Y.; Choi, W.-Y.; Kwak, H.-Y. Thermoeconomic analysis of an ocean thermal energy conversion plant. *Renew. Energy* **2016**, *86*, 1086–1094. [CrossRef]
7. Thirugnana, S.T.; Jaafar, A.B.; Rajoo, S.; Azmi, A.A.; Karthikeyan, H.J.; Yasunaga, T.; Nakaoka, T.; Kamyab, H.; Chelliapan, S.; Ikegami, Y. Performance Analysis of a 10 MW Ocean Thermal Energy Conversion Plant Using Rankine Cycle in Malaysia. *Sustainability* **2023**, *15*, 3777. [CrossRef]
8. Langer, J.; Quist, J.; Blok, K. Upscaling scenarios for ocean thermal energy conversion with technological learning in Indonesia and their global relevance. *Renew. Sustain. Energy Rev.* **2022**, *158*, 112086. [CrossRef]
9. Langer, J.; Cahyaningwidi, A.A.; Chalkiadakis, C.; Quist, J.; Hoes, O.; Blok, K. Plant siting and economic potential of ocean thermal energy conversion in Indonesia a novel GIS-based methodology. *Energy* **2021**, *224*, 120121. [CrossRef]

10. Halimi, B.; Atolah, R.Y. Analysis of 100 kW ocean thermal power plant with butene as working fluid. *IOP Conf. Ser. Earth Environ. Sci.* **2019**, *339*, 012039. [CrossRef]
11. Ou, F.; Ning, B.; Li, J.; Tian, Y.; Qiu, D.; Geng, L.; Jin, X. Design, construction and sea trials of the 20 kW ocean thermal energy conversion in the South China Sea. *Energy* **2026**, *342*, 139641. [CrossRef]
12. Xiang, S.; Cao, P.; Erwin, R.; Kibbee, S. OTEC Cold Water Pipe Global Dynamic Design for Ship-Shaped Vessels. In *Proceedings of the ASME 2013 32nd International Conference on Ocean, Offshore and Arctic Engineering, Nantes, France, 9–14 June 2013*; American Society of Mechanical Engineers Digital Collection: New York, NY, USA, 2013. [CrossRef]
13. Zhang, Y.; Zheng, M.; Zhang, L.; Zhang, C.; Tan, J.; Zhang, Y.; Duan, M. Investigation of Dynamic Behavior of Ultra-Large Cold-Water Pipes for Ocean Thermal Energy Conversion. *Dynamics* **2023**, *3*, 468–487. [CrossRef]
14. Adiputra, R.; Utsunomiya, T. Linear vs non-linear analysis on self-induced vibration of OTEC cold water pipe due to internal flow. *Appl. Ocean Res.* **2021**, *110*, 102610. [CrossRef]
15. Adiputra, R.; Utsunomiya, T. Stability based approach to design cold-water pipe (CWP) for ocean thermal energy conversion (OTEC). *Appl. Ocean Res.* **2019**, *92*, 101921. [CrossRef]
16. Li, T.; An, C.; Liang, W.; Duan, M.; Estefen, S.F. Semi-analytical solution for soil-constrained vibration of subsea free-spanning pipelines. *Ships Offshore Struct.* **2018**, *13*, 666–676. [CrossRef]
17. Cao, Y.; Yin, S.; Li, B.; Jia, S.; Li, Y.; Qin, Y.; Hong, R.; Shuai, K. Study on the Mechanism Between Weld Microstructure and Crack Tie Opening Displacement Fracture Toughness of the Steel Catenary Riser. *Materials* **2025**, *18*, 176. [CrossRef]
18. Gu, J.; Ma, T.; Duan, M. Effect of aspect ratio on the dynamic response of a fluid-conveying pipe using the Timoshenko beam model. *Ocean Eng.* **2016**, *114*, 185–191. [CrossRef]
19. Krishnakumari, A.; Saravanan, M.; Vishal, S.; Krishna, A.A.; Kumar, A.S.; Lindsay, S. Modelling and analysis of vortex induced vibration in marine risers. *Mater. Today Proc.* **2023**. [CrossRef]
20. Han, J.; Wang, Z. Analysis of vibration characteristics of deep-sea mining risers under emergency disconnection state. *Appl. Ocean Res.* **2025**, *158*, 104548. [CrossRef]
21. Gao, Y.; Fu, S.; Yang, J.; Wang, M. Fatigue Damage Analysis of Vortex-Induced Vibration of a Long Flexible Riser. *J. Shanghai Jiao Tong Univ.* **2016**, *50*, 1270–1277. [CrossRef]
22. Yin, Z.; Li, Z.; Longchi, Z.; Wang, Y.; Huang, X. A frequency-dependent high-cycle fatigue damage model and its application in crack nucleation of marine riser from corrosion pits. *Fatigue Fract. Eng. Mater. Struct.* **2023**, *46*, 1488–1499. [CrossRef]
23. Sheehan, J.M.; Grealish, F.W.; Harte, A.M.; Smith, R.J. Characterizing the Wave Environment in the Fatigue Analysis of Flexible Risers. *J. Offshore Mech. Arct. Eng.* **2006**, *128*, 108–118. [CrossRef]
24. Habib, M.I.; Adiputra, R.; Prabowo, A.R.; Erwandi, E.; Muhayat, N.; Yasunaga, T.; Ehlers, S.; Braun, M. Internal flow effects in OTEC cold water pipe: Finite element modelling in frequency and time domain approaches. *Ocean Eng.* **2023**, *288*, 116056. [CrossRef]
25. Vega, L.A. Ocean Thermal Energy Conversion. In *Encyclopedia of Sustainability Science and Technology*; Springer: New York, NY, USA, 2012; pp. 7296–7328. [CrossRef]
26. Xiao, C.; Gulfam, R. Opinion on ocean thermal energy conversion (OTEC). *Front. Energy Res.* **2023**, *11*, 1115695. [CrossRef]
27. Fan, C.; Chen, Y. Design Optimization of Ocean Thermal Energy Conversion (OTEC) Considering the Off-Design Condition. *J. Therm. Sci.* **2023**, *32*, 2126–2143. [CrossRef]
28. Firmansyah, A.I.; Mukhtasor Satrio, D.; Rahmawati, S.; Ikhwani, H.; A Pratikto, W. A study of the temperature distribution in the OTEC cold water pipe using a heat and mass transfer approach. *IOP Conf. Ser. Earth Environ. Sci.* **2024**, *1372*, 012018. [CrossRef]
29. Fu, Q.; Zhang, L.; Mao, L.; Zeng, S.; Huang, S. Temperature Distribution of Cold Water Pipe for Ocean Thermal Energy Conversion. *Ocean. Eng. Equip. Technol.* **2022**, *9*, 7–13. [CrossRef]
30. Zhang, J. Study on Flow Drag Reduction and Temperature Rise Characteristics of Deep Seawater Lifting Pipeline. Master's Thesis, Dalian University of Technology, Dalian, China, 2023. [CrossRef]
31. Mao, L.; Wei, C.; Zeng, S.; Cai, M. Heat transfer mechanism of cold-water pipe in ocean thermal energy conversion system. *Energy* **2023**, *269*, 126857. [CrossRef]
32. Holman, J.P. *Heat Transfer*, 10th ed.; McGraw-Hill: New York, NY, USA, 2010.
33. Incroper, F.P.; DeWitt, D.P.; Bergman, T.L.; Lavine, A.S. *Fundamentals of Heat and Mass Transfer*, 6th ed.; John Wiley & Sons: New York, NY, USA, 2006.
34. Zhou, W.; Xu, F.; Tu, S.; Zhang, X.; Ji, Q.; Chen, S.; Zhang, Y. Study on the variation characteristics of near-surface wind field over the South China Sea and its correlation with ENSO. *J. Mar. Meteorol.* **2018**, *38*, 82–90. [CrossRef]
35. Wang, S.; Liang, B. *Wave Mechanics for Ocean Engineering*; China Ocean University Press: Qingdao, China, 2013.